Feature Edge-Detail Preservation of Random-Valued Impulse Noise in Images

Patitapaban Rath, Rajesh Siddavatam, and Pradeep Kumar Mallick

Abstract In this paper, we put forth a progressive, decision-based, two-phase image denoising algorithm for eliminating random-valued impulse noise from images. The manner in which this algorithm deals with noise is a completely pristine method when compared to the other existing image denoising algorithms. In the primary phase, the noise is dealt at a coarse level; in other words, the noisy pixels that are easily differentiable from the neighborhood are eliminated. In the secondary phase, fine-level image denoising is performed. In other words, the left-over fine scale noise in the detected corrupted pixels of the first phase, which cannot be straightforwardly differentiated from the surrounding pixels, is eliminated. In both the phases, separate mechanisms were followed to eliminate noise in the interior regions and edge regions. Hence, the algorithm is edge-detail preserving. Images with very high noise levels, in other words, with 70% noisy pixels were restored successfully. Speaking in terms of quantitative significant measures, the restored images in most cases were better than those of the other existing filters.

Keywords Image denoising · Random-valued impulse noise · Mean structural similarity index (SSIM) · Localized pixel intensity variation (LPIV) filter

P. Rath (✉) · P. K. Mallick
School of Computer Engineering, KIIT University, Bhubaneswar, India
e-mail: pabanrath@gmail.com

P. K. Mallick
e-mail: pradeep.mallickfcs@kiit.ac.in

R. Siddavatam
VVIT, Guntur, India
e-mail: srajesh@ieee.org

M. Chakraborty et al. (eds.), *Trends in Wireless Communication and Information Security*,
Lecture Notes in Electrical Engineering 740,
https://doi.org/10.1007/978-981-33-6393-9_15

1 Introduction

Impulse noise is broadly classified into salt-and-pepper noise and random-valued impulse noise. In images corrupted by salt-and-pepper noise, the noisy pixels can take only the maximum and the minimum values in the dynamic range, while in the images corrupted by random-valued noise (RV noise), they can occupy any value in between the minimum and maximum values in the same dynamic range.

Hence, practically speaking, handling RV noise would be quite tedious. The sources of impulse noise have been explained in [1].

Among the various existing denoising methods, the median filter is used extensively because of its effective noise subduing potential and computational effectiveness. Its denoising power and computational efficiency are elaborated in [3, 4], respectively.

However, the main drawback of a standard median filter is that it is effective only for low-noise densities [5] and the vital original information of the image is lost because it is not a decision-based filter. The other drawback of the median filter was that it was not decision based; in other words, it cannot preserve original information.

In order to ameliorate denoising, many other impulse detector filters were proposed. The weighted median filter [6] and adaptive median-based filters [7] were partially decision based. The adaptive median-based filter using second-generation wavelets [8], multi-state median filter [9], the homogeneous information-based filters [10, 11], the adaptive center-weighted median filter [12], the peak-and-valley filters [13, 14], the signal-dependent filter [15], the iterative method proposed by Luo [16] and other algorithms like [17–21] are decision-based algorithms. Among the two-phase algorithms, the three-state median (TSM) [22], the adaptive center-weighted median (ACWM) [12], the Luo filter [23], the genetic programming (GP) filter [24] are worth stating. The effective detection technique to replace RV noise in images with high noise levels is an open challenge. A partial differential equation-based technique [25] is an interesting method proposed in recent times, which uses a new defined set of controlling functions for impulse noise removal.

As already said, dealing with RV noise is relatively tedious in contrast to salt-and-pepper impulse noise [26].

We hereby propose the localized pixel intensity variation (LPIV) filter which has been proved successfully by Kireeti Bodduna and Rajesh Siddavatam et al. in [27], [28, 29]. The credibility of cardinal splines for interpolation in impulse noise-related problems was again tested by Rajesh Siddavatam et al. in [29].

Our work introduces a two-phase mechanism for random-valued noise removal. In the first stage, the noisy pixels were dealt with at a coarse level. Noise at a very fine level still persists in those detected pixels after the first phase. So in the second phase, for those pixels which were detected as noisy in the first phase, the second part of the proposed algorithm is applied. The fact that edge pixels and interior pixels were separately dealt with in both the phases of the algorithm is the prime reason for edge-detail preservation in the restored images. We make use of dyadic wavelets of canny to determine whether a particular pixel belongs to the interior region or the edge region.

The outline of this paper is as follows: The proposed algorithm and the significant measures are discussed in Sect. 2. The results along with conclusions have been discussed in Sect. 3.

2 Proposed Algorithm

The noise detection job is performed by the LPIV filter [29]. It designates each and every pixel in the window as a noisy pixel or a noise-free counterpart. Once a pixel is detected as noisy, it is replaced by interpolating the noise-free pixels in the neighborhood with cardinal splines. By neighborhood, we mean the particular window in the image where the algorithm is currently active.

2.1 Coarse Level Image Denoising—I

This is the first phase of the algorithm where the noise is removed in local neighborhoods where the noisy pixels can be identified with certainty. "The underlying idea of the localized pixel intensity variation (LPIV) filter is that the gray-scale pixel intensities in a local neighborhood vary insignificantly. Thus, for every central pixel in a window, we find the noise-free pixels in that window. Subsequently, using these noise-free pixels, we calculate a local threshold. Depending on this threshold, we decide the fate of the central pixel whether it is corrupted by noise or not. If corrupted, we replace it by interpolating the noise-independent pixels.

If the center pixel belongs to the interior region of the image, a threshold of T1 + □ is used, where □ is the flexibility parameter for interior regions andis constant for a particular image, but different for various images. Rajesh Siddavatam et al. computational results showed that when it is varied between 20 and 60 dB we obtain better restored images. To be more precise, a particular value of in this range gives best interpolation results as elaborated in [29].

In the second case, if the center pixel belongs to the edge region of the image, a threshold of T1 + □ is used, where □ is the flexibility parameter for edge regions [29].

The novelty here lies in the fact that the threshold selected is a function of the window. In other words, the threshold is calculated locally but not globally like in some of the erstwhile proposed filters. This paves way for better detection and hence better restored images.

2.2 LPIV 1 for Interior Regions

INPUT: Coarse scale denoised image $\sum(i, j)$. This algorithm is simulated for only those interior pixels which were detected as noisy in the first phase. Again, we define the 3×3 window $\Omega = \{(s, t)| - 1 \leq s, t \leq 1\}$ centered at (O, O). Here, the center element is the noisy interior pixel detected in phase 1.

Step A:

$$\forall D(i, j) \in \sum(i, j) \in \sum_{1}$$

(For the detected interior region noisy pixels in phase 1).

$Z(1) = \Omega(0,1)$
$Z(2) = \Omega(0, -1)$
$Z(3) = \Omega(-1, 0)$
$Z(4) = \Omega(1, 0)$
$b \leftarrow (-\beta\alpha^3 + 2\,\beta\alpha^2 - \beta\alpha)$
$b \leftarrow [(2 - \beta)^0\alpha^3 + (\beta - 3)\alpha^2 + 1]$
$b \leftarrow [(\beta - 2)^1\alpha^3 + (3 - 2\beta)\alpha^2 + \beta\alpha]$
$b \leftarrow (\beta\alpha^3 + {}^2\beta\alpha^2)$
$pt. = b_0 * Z({}^3 1) + b_1 * Z(2) + b_2 * Z(3) + b_3 * Z(4)$
$\Omega(0,0) = pt.$
OUTPUT: Interior region fine scale denoised image $\sum(i, j)$.

2.3 LPIV 2 for Edge Regions

INPUT: Interior region fine-level denoised image $\sum(i, j)$. This algorithm is simulated for only those edge pixels which were detected as noisy in the first phase. Again, we define the 3×3 window $\Omega = \{(s, t)|-1 \leq s, t \leq 1\}$ centered at (0, 0). Here the center element is the noisy edge pixel detected in phase 1.

Step B:

$$\forall D(i, j) \in \sum (i, j) \in \sum_{2}$$

- $Z(1) = \Omega(0,1)$
- $Z(2) = \Omega(0, -1)$
- $Z(3) = \Omega(-1, 0)$
- $Z(4) = \Omega(1, 0)$
- $b \leftarrow (-\beta\alpha^3 + 2\,\beta\alpha^2 - \beta\alpha)$
- $b \leftarrow [(2-\beta)^0\alpha^3 + (\beta - 3)\alpha^2 + 1]$
- $b \leftarrow [(\beta - 2)^1\alpha^3 + (3 - 2\beta)\alpha^2 + \beta\alpha]$
- $b \leftarrow (\beta\alpha^3 + {}^2\beta\alpha^2)$
- $pt. = b_0 * Z({}^3 1) + b_1 * Z(2) + b_2 * Z(3) + b_3 * Z(4)$
- $\Omega(0,0) = pt$
- OUTPUT: Edge region fine scale denoised image $\sum (i, j)$. The image $\sum (i, j)$ is the final restored image (Table 1; Fig. 1).

3 Results and Conclusions

Figures 2, 3, 4 and 5 show the final restored images from various noise levels of Lena, Bridge, Peppers and Airplane. Tables 2, 3 and 4 give the comparative analysis with other existing algorithms. The PSNR values are quite impressive keeping in mind the corresponding amount of noise 60% in the original images.

Summarizing the results from the above figures, it can be clearly seen that when the noise density increases, the PSNR and MSSIM values decrease. As the noise density increases, the amount of original information that is available to us decreases. The standard test images were procured from the University of Southern California image database. All the images were 8-bit images with dynamic ranges from 0 to 255. Peak signal-to-noise ratio (PSNR) and structural similarity index measure (SSIM) [32] have been used as quantitative yardsticks to measure the restored images.

Table 1 Parametric values used in the initial iteration of both LPIV 1 and LPIV 2 for various images

Image	α	B	γ (dB)	δ (dB)
Lena	0.5	−1.8	25.0	32.5
Bridge	0.4	−2.3	45.0	60.0
Peppers	0.5	−1.8	25.0	32.5
Airplane	0.4	−2.5	32.5	47.5
Bridge	0.5	−2.1	25.0	62.5

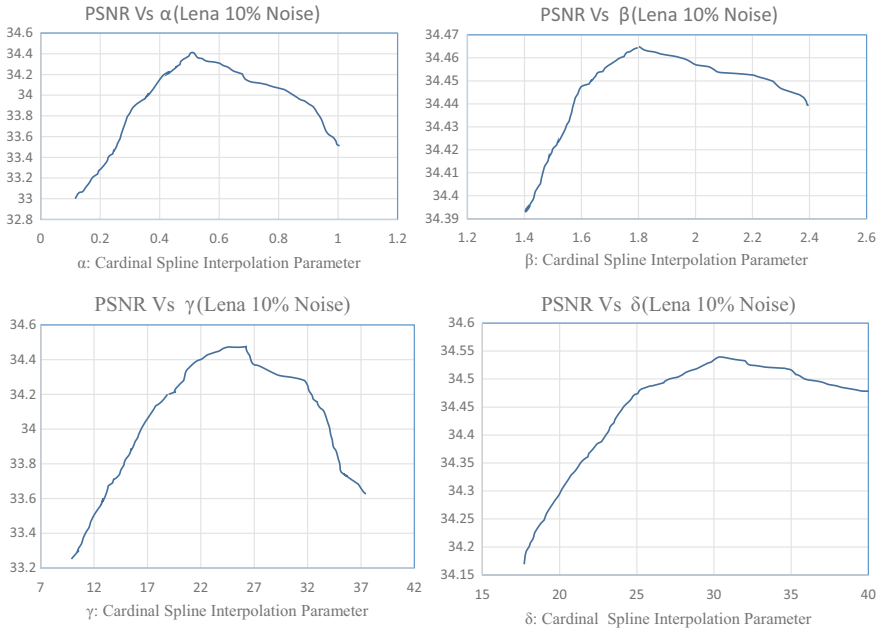

Fig. 1 Parameter optimization for Lena image to obtain optimal PSNR by varying α, β

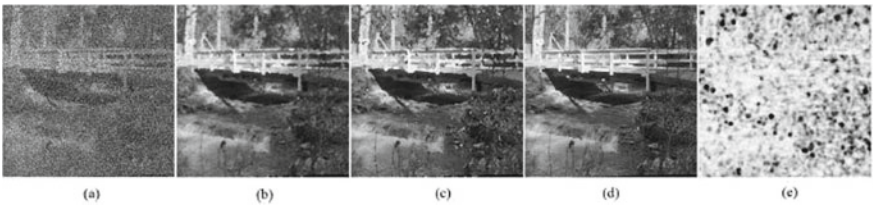

Fig. 2 **a** Noisy image Lena: 60%, **b** LPIV1 (25.96 dB), **c** LPIV2 (25.90 dB), **d** original image, **e** SSIM Map (MSSIM = 0.8906)

Fig. 3 **a** Noisy Bridge: 60%, **b** LPIV1 (21.4 dB), **c** LPIV2 (22.57 dB), **d** original image, **e** SSIM map (MSSIM = 0.7886)

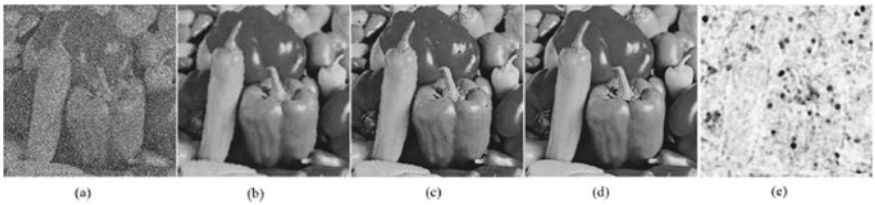

Fig. 4 **a** Noisy Peppers: 60%, **b** LPIV1 (24.99 dB), **c** LPIV2 (22.14 dB), **d** original image, **e** SSIM map (MSSIM = 0.8448)

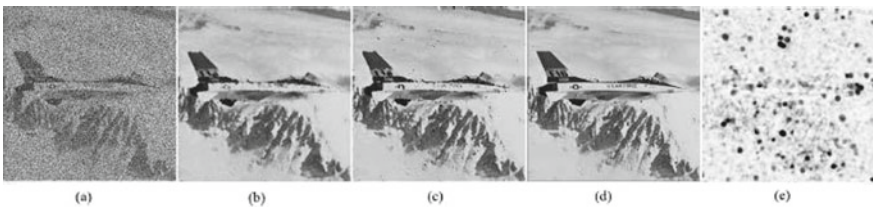

Fig. 5 **a** Noisy Airplane: 60%, **b** LPIV1 (23.76 dB), **c** LPIV2 (24.7 dB), **d** original image, **e** SSIM map (MSSIM = 0.8719)

The proposed localized pixel intensity variation (LPIV) filter has two-way mechanism of denoising random-valued impulse noise, and it has been found that the obtained restored images are either superior to those produced by other theoretical models in most cases or almost similar to the results of other works in a very few cases. When compared with other algorithm results (Tables 2, 3, 4 and 5), in a total of 30 cases, in 20 cases LPIV (either LPIV1 or LPIV2) gave best results and in 7 cases, PDE (NSDD + NTVD) gave better results while in only 3 cases GP gave best results. Another advantage of using this method is that it does not involve any time-consuming theoretical equations. Hence, the computational efficiency is impressive. Finally, our proposed methodology also suffices for color images (by extending the LPIV to three dimensions). Future work can be done in applying this filter to 3D mesh models and point cloud graphic models.

Table 2 Comparison of PSNR (dB) of restored images using different algorithms for Lena image

Noise (% age)	LPIV2	LPIV1	PM	NPM	SDD	NSDD	TVD	NTVD	-	-
10	37.66	34.56	23.5	28.7	29.9	32.8	25.4	32.9	-	-
20	34.86	31.56	21.7	28	28.7	31.4	23.1	31.2	-	-
30	32.47	30.7	20	27.1	26.3	29.9	20.9	29.4	-	-
Noise (% age)	LPIV2	LPIV1	NSDD	MED(5×5)	MED(7×7)	TSM(5×5)	TSM(7×7)	ACWM	Luo	GP
40	29.32	29.64	28.35	25.97	25.35	26.48	25.78	26.47	28.27	28.13
50	27.59	27.79	26.39	23.1	23.46	23.3	23.66	22.84	26.23	24.86
60	25.9	25.95	24.08	20.25	21.04	20.29	21.12	19.92	24.21	21.68
70	23.95	24.9	–	–	–	–	–	–	–	–

Table 3 Comparison of PSNR (dB) of restored images using different algorithms for Bridge image

Noise percentage	LPIV2	LPIV1	PM	NPM	SDD	NSDD	TVD	NTVD
10	***32.43***	**27.78**	21	24.4	24.5	27.4	22.2	26.8
20	***28.9***	**25.36**	20	23.8	24.1	26.4	21.1	25.8
30	***25.66***	**24.53**	19	23.2	23	25.4	19.8	24.8

Noise %	LPIV2	LPIV1	NSDD	MED (5 × 5)	MED (7 × 7)	TSM (5 × 5)	TSM (7 × 7)	ACWM	Luo	GP
40	**23.61**	**23.57**	23.95	22.25	21.59	22.75	21.97	23.11	23.75	*24.24*
50	***23***	**22.52**	22.65	20.97	20.76	21.24	20.999	21.07	22.52	22.43
60	***22.56***	**21.4**	21.12	19.19	19.45	19.28	19.55	18.67	20.95	20.23
70	***21.86***	**20.23**	–	–	–	–	–	–	–	–

Table 4 Comparison of PSNR (dB) of restored images using different algorithms for Peppers image

Noise percentage	LPIV2	LPIV1	PM	NPM	SDD	NSDD	TVD	NTVD
10	**34.16**	**29.53**	24.1	30.4	31.5	32.4	26.5	34.5
20	**31.45**	**28.32**	22.3	29.4	29.9	31.4	23.9	*32.5*
30	**29.47**	**27.77**	20.6	28.1	27.3	29.9	21.6	*30.1*

Noise%	LPIV2	LPIV1	NSDD	MED(5 × 5)	MED(7 × 7)	TSM(5 × 5)	TSM(7 × 7)	ACWM	Luo	GP
40	**27.66**	**27.01**	*28.89*	26.34	25.87	26.76	26.24	26.81	28.19	28.42
50	**26.31**	**26.12**	*27.02*	24.27	24.52	24.47	24.72	23.89	26.94	25.91
60	***25.14***	**24.98**	24.83	21.22	22.07	21.32	22.13	20.76	24.67	22.71
70	***24.21***	**23.55**	–	–	–	–	–	–	–	–

Table 5 Comparison of PSNR (dB) of restored images using different algorithms for Airplane image

Noise percentage	LPIV2	LPIV1	PM	NPM	SDD	NSDD	TVD	NTVD
10	***33.8***	**28.42**	22.7	28.4	30.3	32.8	25.2	33.5
20	***31.33***	**27.13**	20.9	27.4	28.9	31.1	22.5	31.3
30	***29.42***	**26.07**	19.2	26.6	26.6	29.5	20.1	29

Noise%	LPIV2	LPIV1	NSDD	MED(5 × 5)	MED(7 × 7)	TSM(5 × 5)	TSM(7 × 7)	ACWM	Luo	GP
40	**27.04**	**25.42**	27.62	25.5	24.7	25.88	24.98	25.9	26.92	*27.74*
50	**25.58**	**24.81**	*25.85*	23.22	23.64	23.42	23.82	23.13	25.84	25.23
60	***24.69***	**23.76**	23.96	19.93	21.13	20	21.24	19.67	23.84	21.71
70	***22.8***	**22.37**	–	–	–	–	–	–	–	–

References

1. Gonzalez RC, Woods RE (2002) Digital image processing. Prentice-Hall, Englewood Cliffs
2. Pratt WK (1975) Median filtering. Technical report, Image processing Institute, University of Southern California, Los Angeles, Sept 1975
3. Bovik A (2000) Handbook of image and video processing. Academic, New York
4. Huang TS, Yang GJ, Tang GY (1979) Fast two-dimensional median filtering algorithm. IEEE Trans Acoustics Speech Signal Process ASSP–1(1):13–18
5. Srinivasan KS, Ebenezer D (2007) A new fast and efficient decision based algorithm for removal of high-density impulse noises. IEEE Signal Process Lett 14(3):189–192
6. Brownrigg D (1984) The weighted median filter. Commun Assoc Comput 807–818
7. Hwang H, Haddad RA (1995) Adaptive median filters: new algorithms and results. IEEE Trans Image Process 4(4):499–502
8. Syamala Jaya Sree P, Kumar P, Siddavatam R, Verma R (2013) Salt-and-pepper noise removal by adaptive median-based lifting filter using second-generation wavelets. Signal Image Video Process 7(1):111–118
9. Chen T, Wu HR (2001) Space variant median filters for the restoration of impulse noise corrupted images. IEEE Trans Circuit Syst II Analog Digit Signal Process 48(8):784–789
10. Eng H-L, Ma K-K (2001) Noise adaptive soft-switching median filter. IEEE Trans Image Process 10(2):242–251
11. Pok G, Liu J-C, Nair AS (2003) Selective removal of impulse noise based on homogeneity level information. IEEE Trans Image Process 12(1):85–92
12. Chen T, Wu HR (2001) Adaptive impulse detection using center-weighted median filters. IEEE Signal Process Lett 8(1):1–3
13. Windyga PS (2001) Fast impulsive noise removal. IEEE Trans Image Process 10(1):173–179
14. Alajlan N, Kamel M, Jernigan E (2004) Detail preserving impulsive noise removal. Signal Process Image Commun 19:993–1003
15. Abreu E, Lightstone M, Mitra SK, Arakawa K (1996) A new efficient approach for the removal of impulse noise from highly corrupted images. IEEE Trans Image Process 5(6):1012–1025
16. Luo W (2005) A new efficient impulse detection algorithm for the removal of impulse noise. IEICE Trans Fundam E88-A(10):2579–2586
17. Syamala Jaya Sree P, Raj P, Kumar P, Siddavatam R, Ghrera SP (2013) A fast novel algorithm for salt and pepper image noise cancellation using cardinal B-splines. Signal Image Video Process 7(6):1145–1157
18. Aizenberg I, Butakoff C, Paliy D (2005) Impulsive noise removal using threshold Boolean filtering based on the impulse detecting functions. IEEE Signal Process Lett 12(1):63–66
19. Besdok E, Yksel ME (2005) Impulsive noise suppression from images with Jarque-Bera test based median filter. Int J Electron Commun 59:105–110
20. Crnojevic V, Senk V, Trpovski Z (2004) Advanced impulse detection based on pixel-wise MAD. IEEE Signal Process Lett 11(7):589–592
21. Russo F (2004) Impulse noise cancellation in image data using a two-output nonlinear filter. Measurement 36:205–213
22. Chen T, Ma K-K, Chen L-H (1999) Tri-state median-based filters in image denoising. IEEE Trans Image Process 8(12):1834–1838
23. Luo W (2007) An efficient algorithm for the removal of impulse noise from corrupted images. Int J Electron Commun 61(8):551–555
24. Petrovic N, Crnojevic V (2008) Universal impulse noise filter based on genetic programming. IEEE Trans Image Process 17(7):1109–1120
25. Jian Wu, Tang C (2011) PDE-based random-valued impulse noise removal based on new class of controlling functions. IEEE Trans Image Process 20(9):2428–2438
26. Ghanekar U, Singh AK, Pandey R (2010) A contrast enhancement based filter for removal of random valued impulse noise. IEEE Signal Process Lett 17(1):47–50

27. Bodduna K, Siddavatam R (2012) A novel algorithm for detection and removal of random valued impulse noise using cardinal splines. In: 2012 Annual IEEE proceedings of India conference (INDICON), Dec 2012, pp 1003–1008
28. Bodduna K (2013) A novel algorithm for random-valued-impulse noise detection and removal using Chebyshev polynomial interpolation. In: Proceedings of second IEEE international conference on image information processing (ICIIP), Dec 2013, pp 410–415
29. Jayasree S, Bodduna K, Pattnaik PK, Siddavatam R (2014) An expeditious cum efficient algorithm for salt-and-pepper noise removal and edge-detail preservation using cardinal spline interpolation. J Vis Commun Image R 25:1349–1365
30. Unser M (1999) Splines: a perfect fit for signal and image processing. IEEE Signal Process Mag 16(6):24–38
31. Unser M, Aldroubi A, Eden M (1991) Fast B-spline transforms for continuous image representation and interpolation. IEEE Trans Pattern Anal Mach Intell 13(3):277–285
32. Wang Z, Bovik AC, Sheikh HR, Simoncelli EP (2004) Image quality assessment from error visibility to structural similarity. IEEE Trans Image Process 13(4):600–612